Influence of magnetic Landau damping on the skin effect and Doppler-shifted cyclotron resonance in a metal plate

I. F. Voloshin, N. A. Podlevskikh, V. G. Skobov, L. M. Fisher, and A. S. Chernov

V. I. Lenin All-Union Electrotechnical Institute

The penetration of radiowaves into a plate of compensated metal in an oblique magnetic field is analyzed. The impedance of cadmium, tungsten, and molybdenum plates oriented with their normal parallel to the high-order crystallographic axis is studied experimentally. The rf field distribution in a semiinfinite metal is calculated theoretically with allowance for diffuse reflection of carriers from the boundary and for magnetic Landau damping, which makes the conductivity anisotropic. Expressions are also found for the impedance and the field distribution inside the plate. Because of the anisotropic conductivity, there are two inequivalent directions in the plane of the plate, and the penetration depths of the corresponding longwave components are found to be different. This results in an experimentally observable anisotropy in the smooth impedance of the plate which depends strongly on the inclination angle of the field. The oscillating component of the impedance also becomes anisotropic because of the interaction between the longwave and shortwave field components when the carriers are reflected nonspecularly. Doppleron oscillations are observed for both circular polarizations of the excitation fields, although the Doppler wave remains circularly polarized. The reasons for the experimentally observed decrease of the amplitude of the Gantmakher-Kaner oscillations in an inclined field and the dependence on the inclination angle are discussed. The main experimental results can be explained within the framework of the theory presented here.

Lavrova *et al.*[1] have studied how magnetic Landau damping influences the propagation of dopplerons. The damping decreases the amplitude of the doppleron oscillations in the impedance of a metal plate, and the theory predicts that the damping should be greatest near the lower doppleron threshold H_L. However, the experimental results indicate that the oscillation amplitude actually decreases significantly for a wide range of magnetic fields. The temperature dependence of the oscillations in the impedance of cadmium in an oblique magnetic field has been found to be nonmonotonic,[2] and this behavior also remains unexplained. The theory in Ref. 1 rests on the assumption that carrier reflection from the surface of the plate is perfectly specular, although subsequent measurements have demonstrated that this is false. Indeed, it was shown in Ref. 3 that nonspecular reflection plays a key role and radically alters the properties of the Doppler-shifted cyclotron resonance (DSCR) in metal plates. For diffuse carrier reflection, the amplitudes of the shortwave field components depend on the penetration depth of the longwave component. In addition, the signal picks up an extra gain because of the skin layer that forms when the shortwave components are reflected from the opposite surface of the plate. Moreover, according to Ref. 4 the same conclusion holds for metals with open orbits, for which the conductivity is highly anisotropic in the plane of the plate. In this case both the smooth and the oscillating components of the impedance tensor will differ for the two linear polarizations of the long-wave radiation.

It seems plausible that the unexplained behavior of the impedance oscillations in oblique fields might also be associated with diffuse reflection and with the anisotropic conduction caused by the oblique field. In the present work we analyze the impedance of a metal plate in an oblique magnetic field. The experiments were carried out on cadmium, tungsten, and molybdenum plates; the theoretical analysis is based on the technique developed in Ref. 4, which makes it possible to calculate the field distribution in metals with anisotropic conduction and diffuse carrier reflection. The numerical calculation was carried out using the model Fermi surface for cadmium suggested in Ref. 5. The resulting theory successfully accounts for the experimentally observed behavior of the impedance in oblique fields. The experimental measurements are discussed in Sec. 1; in Sec. 2 we discuss the theory and compare its predictions with the experimental results.

1. EXPERIMENT

We measured the surface impedance $Z = R - iX$ of Cd, W, and Mo single-crystal plates in a constant magnetic field H. The crystals were cleaved in an electric arc from single-crystal ingots and were then chemically treated. The resistance ratio $\rho_{300}/\rho_{4.2}$ at 300 and 4.2 K was 50,000 for the cadmium and tungsten ingots and 30,000 for the molybdenum ingot. The [0001] crystallographic axis for Cd and the [001] axis for W and Mo coincided to within 1° with the normal **n** to the surface of the plates. The plate thicknesses were 1.71, 0.79, and 0.60 mm for cadmium, 2.03 mm for tungsten, and 0.48 and 1.38 mm for molybdenum.

We used an amplitude bridge and autodyne to measure Z. The electromagnetic field was generated by a pair of crossed coils into which the plate was inserted. One of the coils provided the inductance required in the autodyne or bridge circuit. Both coils were wound on a brass form, which ensured that their impedance was virtually independent of the constant magnetic field when no plate was present. The field polarization was continuously selectable from linear to

circular; the doppleron signal in a perpendicular magnetic field was used to select the circular polarization. The impedance oscillations were measured by modulating the field H at 9 Hz and selecting the second-harmonic signal V_2. The field H was generated either by an electromagnet or by a superconducting solenoid. The field orientation (along [0001] for Cd and [001] for W and Mo) was chosen from the condition that the angular dependence of the amplitude and oscillation period be as symmetric as possible; this reduced the error in aligning the field H to less than 0.2°.

For a field $H \parallel$ [0001] and the "minus" circular polarization, the electron doppleron causes distinct oscillations in Z for cadmium. The measurements revealed that when H was oriented away from the [0001] axis, oscillations associated with the electron doppleron also occurred for the "plus" polarization. The amplitude ratio A_+/A_- for these polarizations increased with the field inclination angle ϕ. Figure 1 shows traces for the $-$ (curve 1) and $+$ polarizations (curve 2) for $\phi = 4°$. We found that for the $+$ polarization, the voltage ratio for the excitation coils could be chosen to produce an elliptically polarized field for which the doppleron signal was almost absent (curve 3). Similar (but considerably weaker) effects were noted for the tungsten and molybdenum plates. In what follows we will therefore discuss the oblique-field measurements for the case of cadmium.

It was convenient to use linearly polarized fields when measuring the slowly varying and the oscillating components $\mathscr{F} = \mathscr{R} - i\mathscr{H}$ and ΔZ of the impedance, which were found to be quite sensitive to the angle between H and the axis of the measuring coil. In what follows we will write ϕ for the angle between H and a plane containing the axis of the receiving coil and use ε to denote the angle in the perpendicular plane; quantities measured in these two planes will be denoted by the subscripts ϕ, ε, respectively, while values for a perfectly aligned field $H \parallel$ [0001] are denoted by a 0 subscript. The impedance is more sensitive to changes in ϕ than to changes in ε. Also, there was little change in the observed behavior when the plate was rotated in the receiving coil about the [0001] axis.

We first discuss how the smooth component of the impedance depended on the field inclination. Figure 2 plots the surface resistance $R(H)$ (curves 2,2') and reactance $X(H)$ (curves 1,1') for $H \parallel$ [0001] (curves 1, 2) and for $\phi = 4°$ (curves 1', 2'). (The vertical and horizontal scales for the traces $R(H)$ and $X(H)$ were chosen under the assumption that the maximum value of the slowly varying component of the surface resistance (reached at $H = H_M$) is equal to the smooth component of the reactance: $\mathscr{R}(H_M) = \mathscr{H}(H_M)$. We see that the impedance is sensitive to ϕ for nearly all fields H. The data in Fig. 2 also imply that $|\mathscr{F}|$ decreases with the inclination of the field. Thus, for fields $H \approx 5$ kOe corresponding to maximum oscillation amplitude, $|\mathscr{F}_\phi|$ at $\phi = 4°$ is just $\approx 66\%$ of the value for $H \parallel$ [0001]. For small ϕ and fixed H, $|\mathscr{F}_\phi|$ decreased as ϕ^2 for our sample plates.

The curves $\mathscr{R}_0(H)$ and $\mathscr{R}_\phi(H)$ are qualitatively similar and can be superposed by a linear change of scale of the field variable, namely, $H' = k(\phi)H$. In strong fields, for which $\mathscr{H}(H)$ becomes comparable to $\mathscr{R}(H)$, the curves $\mathscr{H}_0(H)$ and $\mathscr{H}_\phi(H)$ coincide approximately after a change of scale by the same factor $k(\phi)$. The value of $k(\phi)$ can be found from the shift in H_M for which $\mathscr{R}_\phi(H)$ is a maximum:

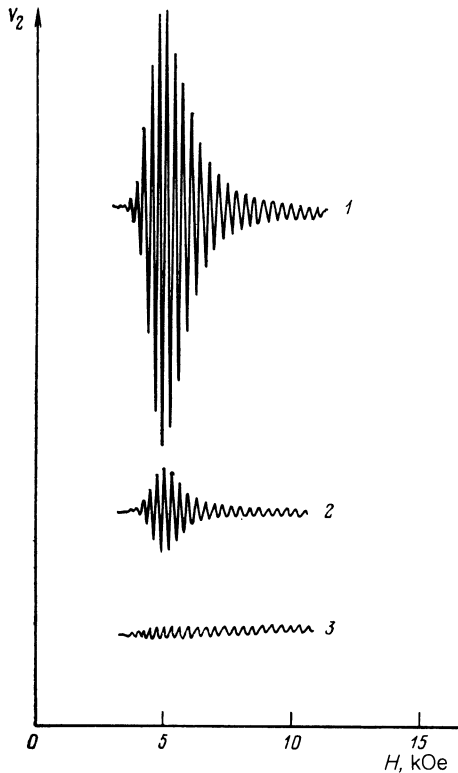$$k(\varphi) = H_M(\varphi)/H_M(0).$$

FIG. 1. Oscillations in the surface resistance of a cadmium plate in an oblique magnetic field (plate thickness $d = 1.71$ mm, frequency $f = 146$ kHz, temperature $T = 1.6$ K).
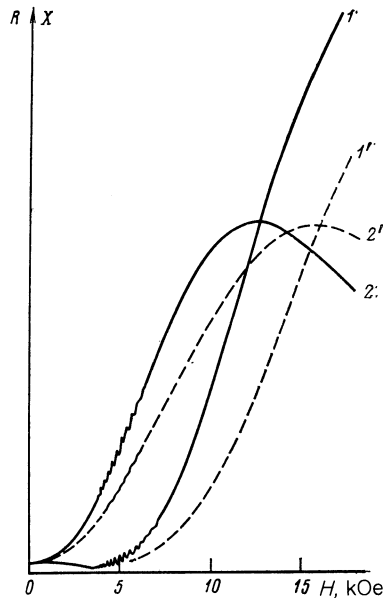

FIG. 2. The dependences $R(H)$ (2,2') and $X(H)$ (1,1') for a cadmium plate ($d = 1.71$ mm, $f = 146$ kHz) for aligned (1,2) and oblique (1',2') fields.

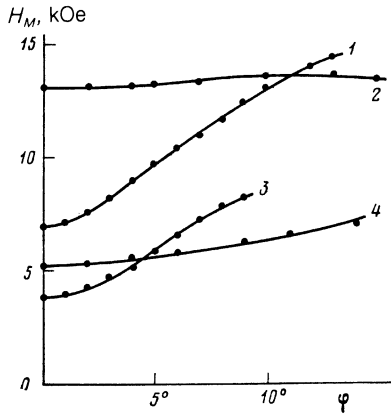204   Sov. Phys. JETP **63** (1), January 1986

Voloshin *et al.*   204

FIG. 3. Field H_M versus angle ϕ for cadmium plates of various thickness ($d = 1.71$ mm for curves 1, 2, and $d = 0.60$ mm for curves 3, 4) for two temperatures: $T = 1.6$ K (1,3) and $T = 4.2$ K (2,4); $f = 146$ kHz.

Figure 3 illustrates how H_M (ϕ) depends on ϕ, the field inclination in the ϕ direction. The measurements were made at 1.6 and 4.2 K for two plates of widely differing thicknesses d. The shift in H_M (ϕ) toward higher fields was much greater at the lower temperature, particularly for the thick sample. On the other hand, the relative change $\Delta H_M/H_M$ was greater for the thin sample at both temperatures. In all cases, a nearly quadratic dependence ΔH_M $(\phi) \propto H_M$ $(0)\phi^2$ was found for $\phi \leqslant 4°$. The coefficient $k(\phi)$ was insensitive to changes in the field frequency.

Deviations of the magnetic field by an angle $\varepsilon \lesssim 15°$ in the perpendicular plane do not significantly alter the slowly varying components of the impedance. Thus, under the conditions indicated in the caption to Fig. 2, $\mathscr{R}_\varepsilon$ (H) and $\mathscr{H}_\varepsilon$ (H) for $\varepsilon = 4°$ coincide to within the $\sim 1\%$ error with curves 1 and 2 in Fig. 2, which correspond to $H \| [0001]$. Although H_M decreases somewhat as ε increases, $\Delta H_M(\varepsilon)$ $\ll \Delta H_M(\phi)$ for equal angles ϕ and ε.

Figure 4 illustrates how the oscillations in the surface resistance change in an oblique field. We see that for equal angles ϕ and ε, the oscillations decrease more rapidly for a field inclined in the ϕ direction.

The measurements imply that when the excitation field is linearly polarized, the behavior of the oscillation amplitude depends on the change in the smooth impedance. The dark circles in Fig. 5 show the ratio A_ϕ/A_ε for $\phi = \varepsilon = 4°$. Curves 1 and 2 plot $|\mathscr{F}_\varphi|^2/|\mathscr{F}_\varepsilon|^2$ and $\mathrm{Re}(\mathscr{F}_\varphi^2)/\mathrm{Re}(\mathscr{F}_\varepsilon^2)$, respectively. In weak fields, for which $\mathscr{H}(H) \ll \mathscr{R}(H)$, these curves nearly coincide; their difference becomes appreciable only as H approaches H_M. For a wide range of magnetic fields, the experimental values A_ϕ/A_ε lie close to curve 2. The amplitudes A_ε and A_ϕ are thus related for inclined fields and we need only study one of them.

We also investigated the oscillation amplitude for fields inclined in the ε direction; in this case the smooth component of the impedance remained virtually unchanged. Figure 6 plots $A_\varepsilon/A_0(H)$ for two values of ε; A_ε/A_0 is smallest for H near the lower doppleron threshold, and it increases and saturates with increasing H. Comparison of Figs. 6 and 7 shows that the limiting value of A_ε/A_0 is independent of tempera-
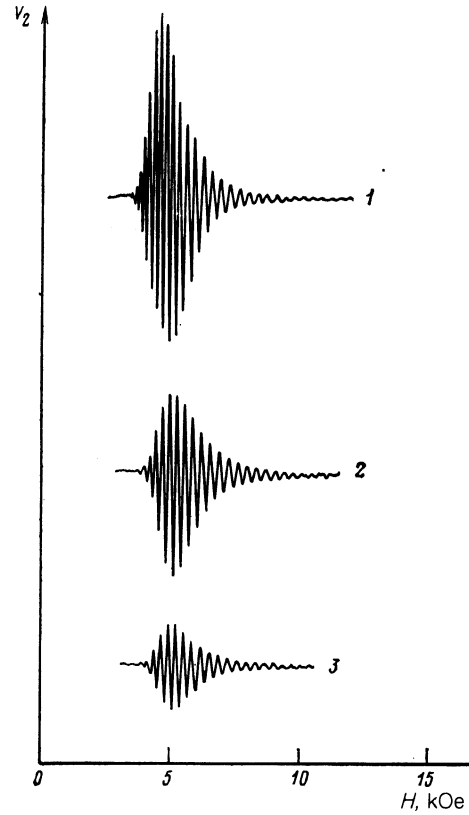

FIG. 4. Traces showing oscillations of the surface resistance of cadmium in perpendicular (curve 1) and inclined magnetic fields for $\varepsilon = 4°$ (curve 2) and $\phi = 4°$ (curve 3); $d = 1.71$ mm, $T = 1.6$ K, $f = 146$ kHz. Curves 2 and 3 were recorded at twice the sensitivity for curve 1.

ture and frequency and depends only on the field inclination angle.

The same qualitative behavior was observed for tungsten and molybdenum, but the plate impedances were less sensitive to the inclination of the field. Unlike the case for cadmium, the (small) change $\Delta H_M(\varepsilon)$ for a field inclined by ε had the same sign as $\Delta H_M(\phi)$.

2. THEORY AND DISCUSSION

1. We use the "lens" model[5] to describe the electron portion of the Cd Fermi surface, according to which the spectrum is of the form

$$\varepsilon(\mathbf{p}) = \frac{1}{2m}\left[p_x^2 + p_{y'}^2 + \frac{4p_0 p_1}{\sigma^2}\sin^2\frac{\sigma p_{z'}}{2p_1}\right], \quad |p_{z'}| < p_F, \quad (1)$$
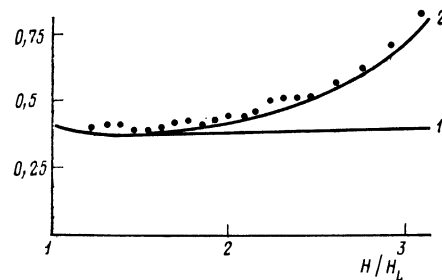

FIG. 5. Measured values of A_ϕ/A_ε (points) and $|\mathscr{F}_\varphi|^2/|\mathscr{F}_\varepsilon|^2$ (curve 1) and $\mathrm{Re}(\mathscr{F}_q^2)/\mathrm{Re}(\mathscr{F}_\varepsilon^2)$ (curve 2) as a function of the magnetic field; $d = 1.71$ mm, $T = 1.6$ K, $f = 270$ kHz.
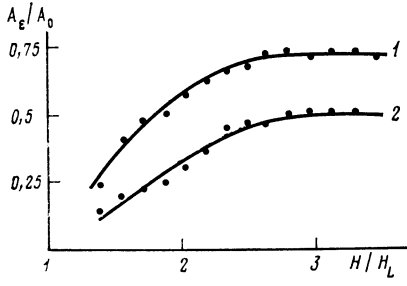
FIG. 6. Behavior of A_ε/A_0 for a cadmium plate of thickness 1.7 mm; $T = 1.6$ K, $f = 140$ kHz. Curve 1 is for $\varepsilon = 4°$, curve 2 for $\varepsilon = 6°$.

$$\varepsilon(\mathbf{p}) = \varepsilon_F \equiv \frac{p_0 p_1}{m(1+\rho)}, \qquad \sigma = (1-\rho^2)^{1/2}, \qquad p_F = \frac{p_1}{\sigma}\arcsin\sigma, \tag{2}$$

where the constant m has the dimensions of mass.

The model parameters ρ, p_0, and p_1 were found in Ref. 5 to be $\rho = 0.2$, $p_0 = 1.5\hbar\text{Å}^{-1}$, and $p_1 = 0.23\hbar\text{Å}^{-1}$, where $\hbar$ is Planck's constant. We take the z' axis to be normal to the plate (parallel to the wave propagation vector $\mathbf{k}$), while the x axis is normal to the plane spanned by $\mathbf{k}$ and $\mathbf{H}$. We will also use an xyz coordinate system with $z\|\mathbf{H}$. The angle between the z and z' axes will be assumed small.

One must know how the electrons move in the inclined magnetic field in order to calculate the nonlocal conductivity tensor. The velocity components of the electrons in the central section of the lens determine the element σ_{xx}^L (the magnetic Landau damping); they are given by

$$v_x(p_z, \Phi) = v_\perp(x)\cos\Phi, \qquad v_y(p_z, \Phi) = v_\perp(x)\sin\Phi,$$

$$v_z(p_z, \Phi) = p_0(\sigma m)^{-1}\sin x + v_\perp(x)\varphi\sin\Phi(p_0 p_1^{-1}\cos x - 1),$$

$$v_\perp(x) = (m\sigma)^{-1}[2p_0 p_1(\cos x - \rho)]^{1/2}, \qquad x = \sigma p_z/p_1, \tag{3}$$

where Φ is the gyrophase of the orbiting electrons. Using these expressions and proceeding as in Ref. 1, we find that

$$\sigma_{xx}^L(q) = \frac{nec}{H}\mu\frac{q^2}{\pi\sigma(1-\rho)^2}\int_{-x_F}^{x_F}\frac{(\cos x - \rho)^2\cos^2 x}{\gamma + iq\sigma^{-1}\sin x}dx, \tag{4}$$

$$\mu = \pi\eta(1-\rho)[2\sigma\lambda(1+\rho)]^{-1}, \qquad \eta = \sigma(p_0/p_1)\varphi^2, \tag{5}$$

$$\lambda = 1 - \rho x_F/\sigma, \qquad x_F = \arcsin\sigma,$$

where $q = kcp_0/eH$ is the dimensionless wave vector; $\gamma = vmc/eH$; n and v are the electron density and the frequency of electron collisions with scattering particles; e is the absolute value of the electron charge, and c is the speed of light. For values $|q| \gg \gamma\sigma_{xx}^L$ has the simple form
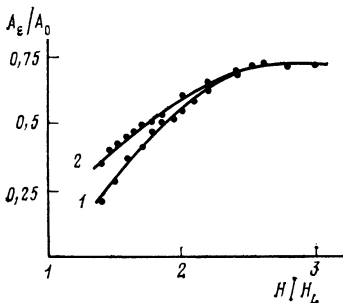

FIG. 7. Dependence of A_ε/A_0 for $T = 1.6$ K (curve 1) and $T = 4.2$ K (curve 2) for a cadmium plate; $d = 1.71$ mm, $f = 260$ kHz.

$$\sigma_{xx}^L(q) = \frac{nec}{H}\mu[(q^2+\gamma^2)^{1/2} - \gamma]. \tag{6}$$

The Hall conductivity $\sigma_{xy}(q)$ cannot be calculated analytically for $\phi \neq 0$. However, if we neglect multiple resonances we can approximate it by the electron conductivity calculated for a Fermi surface axisymmetric with respect to the magnetic field. The primary requirement is that both the volume V and the derivative $(\partial S/\partial p_z)_{ext}$ at the reference point remain constant for this surface; the derivative determines the spatial period of the shortwave field components [$S(p_z)$ is the area of the cross section of the Fermi surface cut by the plane $p_z = \text{const}$]. The conductivity has a resonance singularity which is also important, as it essentially determines the doppleron spectrum. It depends on V and on the derivatives $\partial S/\partial p_z$ and $\partial^2 S/\partial p_z^2$ at the reference point, which are given by

$$V = \frac{4\pi}{\sigma^2}p_0 p_1^2\lambda, \qquad \left(\frac{\partial S}{\partial p_z}\right)_{ext} = -2\pi p_0\left(1+\varphi^2 - \frac{\rho}{\sigma}\eta\right),$$

$$\left(\frac{\partial^2 S}{\partial p_z^2}\right)_{ext} = -\frac{2\pi p_0}{p_1}\left[\rho(1+1.5\varphi^2) + 1.5\frac{\eta}{\sigma}\left(1-2\rho^2 - \frac{\varphi^2}{2}\right)\right] \tag{7}$$

for the initial lens in the inclined magnetic field. We consider a class of model Fermi surfaces whose cross sectional areas are given by

$$S(p_z) = a\frac{2\pi p_0 p_1}{\Sigma^2}\left[\cos\left(b\Sigma\frac{p_z}{p_1}\right) - r\right], \tag{8}$$

where a, b, and r are free parameters, and Λ and Σ are given in terms of r by the same expressions as for λ, σ in terms of ρ. For these models, V, $(\partial S/\partial p_z)_{ext}$, and $(\partial^2 S/\partial p_z^2)_{ext}$ are equal to

$$V = 4\pi p_0 p_1^2\frac{a}{b}\frac{\Lambda}{\Sigma^2}, \qquad \left(\frac{\partial S}{\partial p_z}\right)_{ext} = -2\pi p_0 ab,$$

$$\left(\frac{\partial^2 S}{\partial p_z^2}\right)_{ext} = -2\pi\frac{p_0}{p_1}ab^2r. \tag{9}$$

Equating V, $(\partial S/\partial p_z)_{ext}$, and $(\partial^2 S/\partial p_z^2)_{ext}$ to the values (7) for the original lens model in an inclined magnetic field, we obtain three algebraic equations for a, b, and r. If we assume that ϕ and ρ are small, we find

$$a \approx b \approx 1, \qquad r = \rho + 1.5\eta. \tag{10}$$

Equations (5.7)–(5.9) in Ref. 5, with ρ replaced by r, give the nonlocal conductivity for the model Fermi surface:

$$\sigma_\pm(q) = \pm i\frac{nec}{H}\left[\frac{\varkappa_\pm(q)}{1\pm i\gamma} - \frac{1}{1\mp i\gamma}\right], \tag{11}$$

$$\varkappa_\pm(q) = \frac{1}{2\Lambda t}\ln\frac{1+t}{1-t} + \frac{ir}{2\Lambda(1-r^2-t^2)^{1/2}}\ln\frac{r+i(1-r^2-t^2)^{1/2}}{r-i(1-r^2-t^2)^{1/2}},$$

where $t = q(1 \pm i\gamma)^{-1}$. In what follows we will refer to formulas derived in Refs. 4 and 5, which will be indicated by appending 4 or 5 as a prefix to the equation number.

2. A method was developed in Ref. 4 for calculating the field distribution in a semiinfinite metal or plate with diffusely reflecting surfaces and an anisotropic, nonlocal conductivity. The first step is to calculate the field for a semiinfinite metal; the distribution is given by Eqs. (4.19) and (4.20). One cannot use (4.18) to calculate the surface impedance

directly, because even though the tensors ϕ and τ commute with each other approximately (see Ref. 4), the impedance calculations require the higher (not just the leading) terms in the expansions of τ and ϕ in $1/q$ as $q \to \infty$; the commutator for these terms is negligible only for strong fields ($\xi \ll 4\pi\omega ncp_0^2/eH^3 \ll 1$), for which the α is nearly equal to the identity tensor. This is the situation that was analyzed in Ref. 4; here, however, we are interested in the moderate fields for which dopplerons can exist in cadmium, and the calculations must be carried out to higher order. We rewrite Eq. (4.2) as follows:

$$(q-i\eta)\varphi_2^{-1}\tau_2^{-1}\mathscr{E}_q = -(q+i\eta)^{-1}\varphi_1^{-1}\tau_1^{-1}\alpha^{-1}(\mathscr{E}'+iq\mathscr{E}+\mathscr{F})+\Omega,$$

$$\Omega = (q-i\eta)\varphi_1^{-1}\tau_1^{-1}[\tau_1\varphi_1\varphi_2^{-1}-\varphi_1\varphi_2^{-1}\tau_1]\tau_2^{-1}\mathscr{E}_q,$$

where we adopt throughout the notation introduced in Ref. 4. Expressing $\Omega(q)$ as a difference $\Omega_1(q) - \Omega_2(q)$ of two functions regular in the upper and lower halfplanes, respectively, and moving $\Omega_2(q)$ over to the left-hand side, we obtain an equation whose right- and left-hand sides are regular in the upper and lower half-planes, respectively, and must therefore be constant, equal to the vector $-i\alpha^{-1/2}\mathscr{E}$, say (here we use the fact that $\phi_1^{-1}\tau_1^{-1} \to \alpha^{1/2}$ as $q \to \infty$, where $\alpha = b^{-1}\alpha^{-1/2}b$). The result for the field distribution in a semiinfinite metal is

$$\mathscr{E}(\zeta) = \frac{1}{2\pi i}\int_{-i\tau-\infty}^{-i\tau+\infty}\frac{dq e^{iq\zeta}}{q-i\eta}\tau_2\varphi_2(\alpha^{-1/2}\mathscr{E}-i\Omega_2). \tag{12}$$

Equations (12) and (4.15), (4.17) imply that

$$\mathscr{E}' = i(K+M+A)\mathscr{E},$$

where

$$iA\mathscr{E} = \lim_{q\to\infty}\alpha^{1/2}q\Omega(q).$$

To evaluate this limit we use the explicit formula

$$\Omega_2(q) = -\frac{1}{2\pi}\int_{i\mu-\infty}^{i\mu+\infty}\frac{dz}{z-q}\varphi_1^{-1}\tau_1^{-1}[\tau_1\varphi_1\varphi_2^{-1}-\varphi_1\varphi_2^{-1}\tau_1]$$
$$\times\varphi_2(\alpha^{-1/2}\mathscr{E}-i\Omega_2)$$

for $\Omega_2(q)$. The expression in square brackets vanishes for $|z| \ll 1$, while for $|z| \gtrsim 1$ we can approximate it by the asymptotic expression for the tensor τ_1; the result is

$$\alpha^{1/2}\Omega_2(q) = -\lim_{\zeta\to 0}\frac{1}{2\pi}\int_{i\mu-\infty}^{i\mu+\infty}\frac{dz e^{iz\zeta}}{(z-q)z}[\varphi_1^{-1}K\varphi_1-\varphi_2^{-1}K\varphi_2]$$
$$\times(\alpha^{-1/2}\mathscr{E}-i\Omega_2),$$

where we have used $|K| \ll 1$. The latter inequality implies that $|\Omega_2| \ll \mathscr{E}$, so that the term $-i\Omega_2$ on the right can be discarded.

The second term in square brackets determines the limit of $\alpha^{1/2}q\Omega_2(q)$ as $q \to \infty$, because the first term has no singularities in the upper half-plane. Deforming the path of integration to pass below the pole $z = 0$, we obtain

$$A = \alpha^{1/2}K\alpha^{-1/2} - \lim_{\zeta\to 0}\frac{1}{2\pi i}\int_{-i\delta-\infty}^{-i\delta+\infty}\frac{dz e^{iz\zeta}}{z}\alpha^{1/2}\varphi_2^{-1}K\varphi_2\alpha^{-1/2}.$$

Since the last integral is equal to $-K$, we get the final relation

$$\mathscr{E}' = i(N+M)\mathscr{E}, \tag{13}$$

$$N = \alpha^{1/2}K\alpha^{-1/2}, \tag{14}$$

between $\mathscr{E}'$ and $\mathscr{E}$ which determines the impedance.

Equation (4.23) gives the field distribution $E(\zeta)$ for the longwave component. Although the complete conductivity tensor is antisymmetric, because of the factor α^{-1} this is no longer true of D_L (nor of the tensor K, which relates E to its derivative E' on the surface). However, we will see below that the combination $\alpha^{1/2}K\alpha^{-1/2}$ is antisymmetric, so that the same is of course true for the complete surface impedance tensor.

3. The calculation of the tensor M and the distribution of the shortwave field components associated with the Doppler-shifted cyclotron resonance presents no difficulty in principle. According to Eqs. (4.20), (4.7), (4.14), and (4.16), the expression for the shortwave field components can be written in the form

$$e(\zeta) = W(\zeta)\mathscr{E},$$
$$\overline{W}(\zeta) = \frac{1}{2\pi i}\int_{-\infty}^{\infty}\frac{dq}{q+i\delta}e^{iq\zeta}\overline{D}_R^{-1}(q)\overline{\Psi}_1(q), \tag{15}$$

where as before the overbars denote quantities for circularly polarized radiation. The tensor $q^2\overline{D}_R$ is almost diagonal, and its elements are equal to

$$q^2\overline{D}_R(q) = q^2 - i\xi[\varkappa_\pm(q)-\varkappa_\pm(0)+\tfrac{1}{2}\varkappa_L(q)],$$
$$\varkappa_L = (H/nec)\sigma_{xx}^L(q). \tag{16}$$

We can write (15) as the sum of the residue at the doppleron pole $q = q_2$ plus an integral over the edges of a cut in the q-plane [this integral gives the Gantmakher-Kaner component (GKC)]. The resulting expressions for $\zeta \gg 1$ are identical to the last two terms in (5.9), except that ρ is replaced by r and the additional term $\varkappa_L$ in (16) gives rise to a nonlocal doppleron decay. We can therefore use the results in Ref. 5, where it was noted that except in a small neighborhood of the lower doppleron threshold, the coefficients b_0 and c_0 in (5.9) are given by $-\theta [d(q^2 D_R/dq]_{q=q_2}^{-1}$ and $\pm 1/2$, respectively. Asymptotic expressions for the GKC were found in Ref. 5. For fields well above the upper doppleron threshold, (5.25) implies that the GKC amplitude is proportional to $1/r^2$. It should therefore decrease when the magnetic field is oblique.

To calculate the doppleron amplitude we must numerically solve the dispersion equation $D_R(q) = 0$ and calculate the coefficient b_0. The inclination of the magnetic field has two consequences: 1) The magnetic Landau damping gives rise to an additional doppleron damping, particularly near the lower threshold. 2) The upper doppleron threshold is increased when ρ is replaced by r, and this also decreases the doppleron oscillations. Figure 8 plots the calculated doppleron amplitude $A_{sp}^D = D'^{-1}\exp(iq_2L)$ at the depth $z = d = 1.7$ mm for $\varepsilon = 0$ and $4°$.

The tensor M is insensitive to the inclination of the field—its relative change is comparable to η and may be neglected.
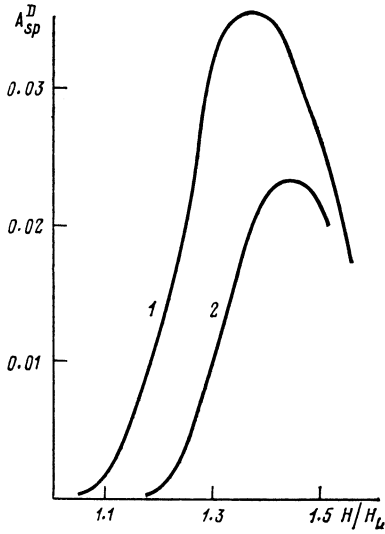
FIG. 8. Calculated dependence of the doppleron oscillation envelopes in a plate ($d = 1.7$ mm) for perpendicular (1) and oblique (2) magnetic fields; $f = 140$ kHz. The carriers were specularly reflected and the mean free path was $l = 2$ mm.

4. Equation (4.23) for the longwave field component takes the form

$$(q^2-q_0^2-i\xi s_L)E_{qx}+i\xi\beta q^2 E_{qy}$$

$$=-(E_x'+iqE_x+F_{qx})-i\xi\beta(E_y'+iqE_y+F_{qy}),$$

$$-i\xi\beta q^2 E_{qx}+(q^2-q_0^2)E_{qy}=i\xi\beta(E_x'+iqE_x)-(E_y'+iqE_y), \quad (17)$$

in Cartesian coordinates, where $q_0 = (1 + i)(\xi\gamma)^{1/2}$ and β_0 is the coefficient of q^2 in the expansion of $\varkappa_{yx}(q)$.

System (17) can be solved in the same way as (4.26), (4.27); the result is

$$E_x(\zeta) = \frac{1}{2\pi i}\int_{-\infty}^{\infty}\frac{dqe^{iq\zeta}}{q-ih}t_2(q)$$

$$\times\left\{E_x-\frac{iC}{q-q_0}[E_y'-i\xi\beta_0 E_x'+iq_0(E_y-i\xi\beta_0 E_x)]\right\}, \quad (18)$$

$$E_y(\zeta)-i\xi\beta_0 E_x(\zeta)$$

$$=\frac{1}{2\pi}\int_{-\infty}^{\infty}\frac{dqe^{iq\zeta}}{q^2-q_0^2}\Big[(E_y'-i\xi\beta_0 E_x')+iq(E_y-i\xi\beta_0 E_x)$$

$$-\frac{\xi\beta_0 q_0^2}{q-ih}t_2(q)\Big\{E_x-\frac{iC}{q-q_0}[E_y'-i\xi\beta_0 E_x'$$

$$+iq_0(E_y-i\xi\beta_0 E_x)]\Big\}\Big], \quad (19)$$

$$C=-i\xi\beta_0 q_0[2(1-\xi^2\beta_0^2)(q_0+ih)t_1(q_0)]^{-1} \quad (20)$$

$$t_{1,2}(q)=\exp\left\{\frac{1}{2\pi i}\int_{-\infty\mp i\delta}^{\infty\mp i\delta}\frac{dz}{z-q}\right.$$

$$\left.\times\ln\frac{[z^2-q_0^2-i\xi\varkappa_L(z)](z^2-q_0^2)-\xi^2\beta_0^2 z^4}{(1-\xi^2\beta_0^2)(z^2+h^2)(z^2-q_0^2)}\right\}. \quad (21)$$

We see from the definition of $t_1(q)$, $t_2(q)$, and C that the pole $q = q_0$ gives no contribution to the distributions (18), (19). The field $E(\zeta)$ must vanish for $\zeta < 0$, as is automatically the case for (18). However, the condition for (19) to vanish requires that the residue of the integrand at $q = -q_0$ must be zero:

$$(E_y'-i\xi\beta_0 E_x')-iq_0(E_y-i\xi\beta_0 E_x)+\frac{\xi\beta_0 q_0^2}{q_0+ih}t_2(-q_0)$$

$$\times\left\{E_x+i\frac{C}{2q_0}[(E_y'-i\xi\beta_0 E_x')+iq_0(E_y-i\xi\beta_0 E_x)]\right\}=0. \quad (22)$$

Upon evaluating expressions (18) and (19) for $\zeta\to 0$ we obtain identities, and the same holds for the ζ-derivative of the function in (19) as $\zeta\to 0$. However, if we take the derivative of (18) we obtain the equation

$$E_x'=iQq_0 E_x+C[(E_y'-i\xi\beta_0 E_x')+iq_0(E_y-i\xi\beta_0 E_x)], \quad (23)$$

$$Q=\frac{-1}{2\pi i q_0}\int dq\ln\frac{[q^2-q_0^2-i\xi\varkappa_L(q)](q^2-q_0^2)-\xi^2\beta_0^2 q^4}{q^2(q^2-q_0^2)(1-\xi^2\beta_0^2)}. \quad (24)$$

Equations (22) and (23) determine the tensor K relating the longwave field component to its derivative on the surface: $E' = iKE$. To calculate the elements of K we use the obvious relation $t_2(-q) = t_1^{-1}(q)$ to express $t_2(-q_0)$ in (22) in terms of C. The tensor N describing the contribution of the long-wave component to the impedance of a semiinfinite metal is then given by

$$N_{xx}=\tfrac{1}{2}q_0[Q+1+(Q-1-2\Delta)G^{1/2}], \quad (25)$$

$$N_{yy}=\tfrac{1}{2}q_0[Q+1-(Q-1-2\Delta)G^{1/2}],$$

$$N_{xy}=-N_{yx}=q_0\left[\frac{2C}{1-C^2G}-\frac{i\xi\beta_0}{2}(Q-1-2\Delta)\right],$$

$$\Delta=2C(i\xi\beta_0+CG)(1-C^2G)^{-1}, \quad G=1-\xi^2\beta_0^2. \quad (26)$$

5. The dispersion equation for the longwave component is

$$[q^2-q_0^2-i\xi\varkappa_L(q)](q^2-q_0^2)-(\beta_0\xi q^2)^2=0. \quad (27)$$

Since in general the solution cannot be found in closed form, we will examine some limiting cases of experimental interest.

a). We first consider the case of intermediate inclination angles ϕ and strong fields H satisfying the inequalities

$$\xi\ll\frac{1}{\mu}|q_0|\ll\frac{1}{\beta_0}. \quad (28)$$

We will not be interested in the small-angle limit, for which $\mu<\beta_0|q_0|$. When (28) holds, the Hall conductivity plays no role and the second term in (27) may be neglected. The long-wave component then has two components with electric fields polarized along the x and y axes, and the dispersion equation has the roots

$$q_x\approx q_0+\tfrac{1}{2}i\xi\mu, \quad q_y=q_0. \quad (29)$$

We see that the magnetic Landau damping due to the inclination of $\mathbf{H}$ has no effect on q_y and changes q_x only slightly.

We next calculate the field distribution in a semiinfinite metal, which is given by Eq. (18). In our case C is small and the function t_2 is of the form

$$t_2(q)=(q-ih)(q+q_0)[q^2-q_0^2-i\mu\xi(q^2+\gamma)^{1/2}]^{-1}. \quad (30)$$

If we substitute (30) into (18) and evaluate the integral in the limit of small and large $q_0\zeta$, we obtain the following interpolation formula:

$$E_x(\zeta) = \left(e^{iq_x\zeta} - \frac{\mu\xi}{\pi q_0}\frac{iq_0\zeta\ln q_0}{1+iq_0\zeta\ln q_0}\frac{1}{1+q_0^2\zeta^2} \right) E_x. \quad (31)$$

The second term in parentheses represents the nonexponential part of the long-wave component of the field caused by the magnetic Landau damping.

Proceeding as in Sec. 4 in Ref. 4 for the case of open orbits, we can use (31) to derive the following expression for the smooth component of the plate impedance:

$$\mathscr{Z}_{xx} = \frac{8\pi\omega d}{c^2}\left(ML + i\left\{ 1 + e^{iq_xL} - \frac{\mu\xi\ln q_0}{\pi q_0} \right.\right.$$

$$\times\left.[1+(1+iq_0L\ln q_0)^{-2}]\right\}$$

$$\times\left[\frac{e^{iq_xL}-1}{iq_xL} - \frac{\mu\xi\ln q_0}{\pi q_0(1+q_0^2L^2)}(1+iq_0L\ln q_0)^{-1}\right]^{-1}\right)^{-1},$$

$$(32)$$

$$M = \frac{1-\rho}{4(1+\rho)\lambda}\xi, \qquad L = \frac{eH}{cp_0}d.$$

The terms containing μ in (32) cause $\mathscr{F}_{xx}$ to depend on the field inclination ($\mu \propto \phi^2$). Calculation shows that the peak in the smooth component of the surface resistance $\mathscr{R}_{xx}$ associated with the Fischer-Kao effect[6] shifts toward higher H as ϕ increases; however, the height of the maximum of $\mathscr{R}_{xx}$ is nearly independent of ϕ. Figure 9 shows results found by calculating the position H_M of the maximum as a function of ϕ. The dependence is very pronounced—even a small inclination of a few degrees suffices to shift H_M substantially. This is due to the shape of the electron "lens" in cadmium: p_0 and p_1 are such that the parameter η in (5) characterizing the magnitude of the magnetic Landau damping is not very small even for small ϕ: $\eta \sim 10\,\phi^2$. We see by comparing Figs. 3 and 9 that the theoretical and experimental results are in qualitative agreement. Moreover, the y-component of the long-wave component (and hence also $\mathscr{F}_{yy}$) is independent of ϕ, again in agreement with experiment.

b). We next consider the case of large angles ϕ, for which

$$\mu\xi \gg |q_0|; \quad (33)$$

we will not assume that the field is strong (so that $\beta_0\xi$ need not be small). The long-wave component is then determined by the magnetic Landau damping, and the corresponding root of the dispersion equation (27) is
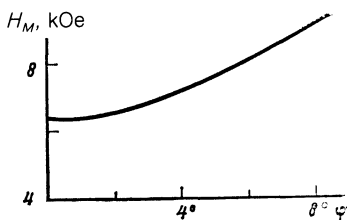
$$q_1 = i\mu\xi(1-\beta_0^2\xi^2)^{-1}, \quad (34)$$

FIG. 9. Dependence $H_M(\phi)$ calculated for $l = 2$mm, $d = 1.7$ mm, $f = 140$ kHz.

where $\beta_0\xi$ differs appreciably from unity. According to (34), the skin layer is much thinner than for case a) and varies as H^2 in strong fields.

As before, C is small; however, Q is now large:

$$Q = -\frac{q_1}{\pi i q_0}\ln q_1. \quad (35)$$

According to (25), the tensor N has the components

$$N_{xx} = {}^{1}/_{2}q_0[Q(1+G^{1/2})+1-G^{1/2}],$$
$$N_{yy} = {}^{1}/_{2}q_0[Q(1-G^{1/2})+1+G^{1/2}], \quad (36)$$
$$N_{xy} = -N_{yx} = -{}^{1}/_{2}q_0 i\xi\beta_0(Q-1).$$

Writing M_+ and M_- for the elements of the tensor M for the two circular polarizations, we find

$$DT_{xx}(0) = M_+ + M_- + q_0Q(1-G^{1/2}) + q_0(1+G^{1/2}),$$
$$DT_{yy}(0) = M_+ + M_- + q_0Q(1+G^{1/2}) + q_0(1-G^{1/2}),$$
$$DT_{xy}(0) = -DT_{yx}(0) = -i[M_+ - M_- - \xi\beta_0 q_0(Q-1)], \quad (37)$$
$$D = 2M_+M_- + q_0(M_+ + M_-)(Q+1)$$
$$-\xi\beta_0 q_0(M_+ - M_-)(Q-1) + 2q_0^2Q$$

for the components of the tensor $T(0)$ which determines the impedance of a semiinfinite metal [see Eqs. (13) and (4.12), (4.13)].

To calculate the impedance of a plate, we must find the field distribution and derive interpolation formulas like the ones for case a). These elaborate formulas will not be given here. In any case, they are not needed for the moderate fields for which the doppleron oscillations exist. Indeed, the plates used in experiments are generally quite thick, so that the Fischer-Kao effect is not observed for the experimental fields, and the continuous component of the plate impedance is just twice the impedance for a semiinfinite metal.

Although $T_{xx}(0)$ and $T_{yy}(0)$ vary because of the Landau damping, they are equal (just as in the absence of damping) at the lower doppleron threshold, where $\xi\beta_0 = 1$. In order to analyze how $T_{xx}(0)$ and $T_{yy}(0)$ behave in stronger fields for which $\xi\beta_0$ is small, we use the fact that $|Q| \gg 1$ and that M_+ and M_- are nearly equal for these fields. It is then clear from (37) that as in case a), the magnetic damping alters $T_{xx}(0)$ appreciably while leaving $T_{yy}(0)$ unchanged. These conclusions are in accord with the measured results.

Let us now consider the oscillating component of the plate impedance, which is given by Eq. (4.63). For fields well above the upper doppleron limit, for which only Gantmakher-Kaner oscillations are observed, the tensor describing the smooth component $\mathscr{F}$ of the impedance is nearly diagonal for both cases a) and b), and the elements $W'_{xx}(L)$ and $W'_{yy}(L)$ are equal. Therefore, as is found experimentally, the ratio $\delta R_{xx}/\delta R_{yy}$ of the oscillation amplitudes is proportional to $\mathrm{Re}(\mathscr{F}_{xx}^2)/\mathrm{Re}(\mathscr{F}_{yy}^2)$. Because the smooth component of the element Z_{yy} is independent of the field inclination, the amplitude of the oscillations in Z_{yy} divided by the corresponding amplitude at zero inclination angle must be equal to $(\rho/r)^2$. For $\varepsilon = 4°$, a calculation using our model gives 0.56, which is fairly close to the experimental value 0.72. If we take $\rho = 0.3$ in the lens model, the calculat-

ed ratios A_ε/A_0 for strong fields and $\varepsilon \lesssim 8°$ agree quantitatively with experiment.

We have already noted that for moderate fields we can replace the smooth component of the plate impedance by twice the impedance of a semiinfinite metal. Since the doppleron has the "minus" circular polarization, the doppleron oscillations in Z_{xx} and Z_{yy} are given by (4.63) as

$$\Delta Z_{xx} = \frac{2\omega u}{c^2} b_0 \exp(iq_2 L) [T_{xx}(0) + iT_{xy}(0)]^2,$$
$$\Delta Z_{yy} = \frac{2\omega u}{c^2} b_0 \exp(iq_2 L) [T_{yy}(0) + iT_{xy}(0)]^2. \tag{38}$$

If $|T_{xy}(0)| \ll |T_{xx}(0) - T_{yy}(0)|$, the second terms in square brackets in (38) can be discarded. This is the case in stronger fields where, as for the Gantmakher-Kaner oscillations, the oscillation amplitudes for the elements Z_{xx} and Z_{yy} are proportional to the squares of the smooth components.

Because $T_{yy}(0)$ is insensitive to the inclination of the magnetic field, the change in the oscillation amplitude ΔZ_{yy} is due to the increase in the collisionless damping of the doppleron and to a change in the doppleron spectrum. On the other hand, the amplitude ΔZ_{xx} decreases further due to the change in the factor $T_{xx}^2(0)$. It is probably not legitimate to neglect $T_{xy}(0)$ at the lower doppleron threshold. However, since $T_{xx}(0) = T_{yy}(0)$ here, the oscillation amplitudes must become equal as the field approaches the lower threshold. All these conclusions are in agreement with the measurements.

Our investigations provide an explanation for the nonmonotonic dependence of the oscillation amplitude in inclined magnetic fields which was observed in Ref. 2. As the temperature drops, the oscillation amplitude changes for a wide range of magnetic fields because of the reduced collisional damping of the shortwave components, and also because the penetration depth of the longwave component of the field is temperature-dependent. The temperature affects the penetration depth in two ways. First, there are fewer collisions, so that the transverse conductivity drops; second, the Landau damping increases the correction to the conductivity [see Eq. (4)] for $q_0 \sim \gamma$. Because of these competing effects, the smooth impedance of the plate varies nonmonotonically, in agreement with Fig. 3, which shows that the impedance may either rise or fall as the temperature decreases. In many case, this nonmonotonic behavior is reflected in a nonmonotonic T-dependence of the oscillation amplitudes. We note that near the lower doppleron threshold, where q_2/γ is not too large, the magnetic Landau damping of the

doppleron wave may depend on temperature, again in agreement with experiment.

We now briefly discuss the behavior of the impedance for a circularly polarized excitation field. The skin-layer field is circularly polarized for $H\|n\|[0001]$ but becomes elliptically polarized in an inclined field. The major axis of the ellipse lies in the inclination plane of the field, and the major/minor semiaxis ratio is close to $\mathscr{R}_\varepsilon/\mathscr{R}_\phi$ for $\mathscr{R} \gg \mathscr{H}$. For example, this ratio is equal to 1.5 (Fig. 2) for an inclination of 4° when H is close to the value H_M corresponding to maximum doppleron oscillation magnitude. A doppleron will be excited if the skin-layer field contains a component with the appropriate circular polarization. Since the skin-layer field is elliptically polarized, it can be represented as a sum of two circularly polarized fields having the same direction of rotation. The ratio $(\mathscr{R}_\varepsilon + \mathscr{R}_\phi)/(\mathscr{R}_\varepsilon - \mathscr{R}_\phi)$ of these fields is equal to 5 for the curves in Fig. 2; it is nearly equal to the ratio of the doppleron oscillation amplitudes for the two polarizations (curves 1 and 2 in Fig. 1).

By changing the voltage applied to the crossed coils by a factor $\mathscr{R}_\varepsilon/\mathscr{R}_\phi$, one can achieve an elliptical polarization for which the skin-layer field is circularly polarized. In this case, for one of the incident wave polarizations no doppleron wave will be excited and no doppleron oscillations will be observed (see curve 3 in Fig. 1). These results provide an experimental demonstration that the doppleron field is circularly polarized in materials with an anisotropic conductivity.

We note in closing that in an oblique magnetic field, the skin-layer field which forms as the doppleron passes through the plate is elliptically polarized. Therefore, even if the excitation is circularly polarized, the signal picked up by the measuring coil will depend on the inclination angle of H and may differ by as much as a factor of $\mathscr{R}_\varepsilon/\mathscr{R}_\phi$.

[1] V. V. Lavrova, V. G. Skobov, L. M. Fisher, A. S. Chernov, and V. A. Yudin, Fiz. Tverd. Tela **15**, 2335 (1973) [Sov. Phys. Solid State **15**, 1558 (1973)].

[2] I. F. Voloshin, L. M. Fisher, and V. A. Yudin, Fiz. Tverd. Tela **20**, 699 (1978) [Sov. Phys. Solid State **20**, 405 (1978)].

[3] I. F. Voloshin, S. V. Medvedev, V. G. Skobov, L. M. Fisher, and A. S. Chernov, Zh. Eskp. Teor. Fiz. **71**, 1555 (1976) [Sov. Phys. JETP **44**, 1814 (1976)].

[4] V. G. Skobov and A. S. Chernov, Zh. Eksp. Teor. Fiz. **87**, 885 (1984) [Sov. Phys. JETP **60**, 502 (1984)].

[5] N. A. Podlevskikh, V. G. Skobov, L. M. Fisher, and A. S. Chernov, Fiz. Tverd. Tela **27**, 330 (1985) [Sov. Phys. Solid State **27**, 202 (1985)].

[6] H. Fischer and Y. H. Kao, Solid State Comm. **7**, 275 (1969).

Translated by A. Mason

210   Sov. Phys. JETP **63** (1), January 1986

Voloshin *et al.*   210